RESEARCH ARTICLE | MAY 23 2024

Exchange coupling in (Co/Pt)$_2$/Nb/(Pt/Co)$_2$ multilayers induced by the Yu–Shiba–Rusinov bound states

Qi Lu ⓘ ; Yaojin Li ⓘ ; Tao Li ⓘ ; Tai Min; Zhuang-De Jiang; Young Sun ⓘ ; Ming Liu ✉ ⓘ

Check for updates

View Online   Export Citation

Articles You May Be Interested In

Spin relaxation and Yu-Shiba-Rusinov states in superconducting graphene

AIP Conference Proceedings (September 2022)

Kinetic coefficients of superconductors with transition-metal impurities

Sov. J. Low Temp. Phys. (September 1976)

Multiple topological phase transitions unveiling gapless topological superconductivity in magnet/unconventional superconductor hybrid platform

Appl. Phys. Lett. (May 2024)

Exchange coupling in (Co/Pt)$_2$/Nb/(Pt/Co)$_2$ multilayers induced by the Yu–Shiba–Rusinov bound states

Qi Lu,[1] Yaojin Li,[1] Tao Li,[2] Tai Min,[2] Zhuang-De Jiang,[3] Young Sun,[4] and Ming Liu[1,a]

AFFILIATIONS

[1]State Key Laboratory for Manufacturing Systems Engineering, Electronic Materials Research Laboratory, Key Laboratory of the Ministry of Education, School of Electronic Science and Engineering, Xi'an Jiaotong University, Xi'an 710049, China
[2]Center for Spintronics and Quantum System, School of Materials Science and Engineering, Xi'an Jiaotong University, Xi'an 710049, China
[3]State Key Laboratory for Manufacturing Systems Engineering, International Joint Laboratory for Micro/Nano Manufacturing and Measurement Technologies, School of Mechanical Engineering, Xi'an Jiaotong University, Xi'an 710049, China
[4]Beijing National Laboratory for Condensed Matter Physics, Institute of Physics, Chinese Academy of Sciences, Beijing 100190, China

[a]Author to whom correspondence should be addressed: mingliu@xjtu.edu.cn

ABSTRACT

The Ruderman–Kittel–Kasuya–Yosida (RKKY) theory of oscillatory exchange interaction in synthetic antiferromagnetic multilayers results in the oscillation behavior of giant magnetoresistance ratio. In addition, the formation of Yu–Shiba–Rusinov (YSR) bound states will induce an extra antiferromagnetic interaction, which is expected to mediate stronger exchange coupling than conventional RKKY interaction. However, the YSR bound states have only been studied in some superconducting hosts with magnetic impurities. The narrow range of material systems that are not compatible with the device integration architecture limits the practical application of YSR interaction. Here, we observe the RKKY interaction and provide the evidence for YSR interaction in Pt/(Co/Pt)$_2$/Nb/(Pt/Co)$_2$/Pt synthetic antiferromagnetic multilayers by quantitatively determining the coupling energy via ferromagnetic resonance technique.

I. INTRODUCTION

Antiferromagnetic materials with exceptional advantages, such as robustness against perturbation, ultrafast dynamics at THz, and considerable spin–orbit effects,[1–6] are promising for future spintronic applications. Despite its merits, the strong direct exchange and small repeat distance limit the application of crystal antiferromagnets in spin-dependent resistance devices. As an alternative, synthetic antiferromagnet (SAF) consists of two magnetic layers with different magnetizations adjacent to the same nonmagnetic spacer layer through the Ruderman–Kittel–Kasuya–Yosida (RKKY) interaction.[7,8] In SAF structures, the weaker exchange coupling allows us to easily manipulate the antiferromagnetic order, which

lays the crucial technical foundation for giant magnetoresistance devices.[9,10] Although SAF structures with RKKY interactions have been extensively explored, the exchange interaction under ultralow temperature has rarely been discussed in the experiment.

Recently, a variety of novel phenomena were investigated in magnetic heterostructures at ultralow temperature regions, such as the superconducting exchange coupling in GdN/Nb/GdN multilayers[11] and an enhanced triplet pure spin supercurrent in Pt/Nb/NiFe/Nb/Pt systems.[12] Here, Nb, a metallic superconductor between two ferromagnetic layers, is widely used to investigate the interplay between ferromagnetism and superconductivity, where superconductivity requires a coupling between antiparallel spin and ferromagnetism emerges from a parallel alignment of spin. In

addition, those two counteractive orders create rich and profound physics in the superconductor/ferromagnet heterostructure, including proximity effect,[13,14] spin-triplet Cooper pairs,[15,16] and superconducting pure spin currents.[17,18] Moreover, the magnetic impurity in the superconducting host induced localized electronic states called Yu–Shiba–Rusinov (YSR) bound states.[19–22] YSR bound states have a spatial extent even more than tens of nanometers[23] and the formation of YSR bound states could significantly enhance antiferromagnetic contribution from indirect spin-exchange.[24] An extra antiferromagnetic coupling channel may occur in Nb-based SAF structures at low temperatures.

This letter demonstrates the YSR interaction in Pt/[Co/Pt]$_2$/ Nb/[Pt/Co]$_2$/Pt heterostructures. The exchange couplings are determined by the ferromagnetic resonance (FMR) technique from room temperature to 4.2 K. We verify the $(k_B T/\varepsilon_F)^2$ relation of bare temperature-dependent RKKY interaction by quantitatively investigating the coupling energy. Moreover, the order of the acoustic mode resonance field and optical mode resonance field reversed at $k_B T < \Delta$, corresponding to a new coupling channel with opposite coupling energy. This result can be clearly explained by an extra antiferromagnetic exchange coupling from the YSR interaction.

II. EXPERIMENTS

Pt (0.9 nm)/[Co (0.75 nm)/Pt (0.9 nm)]$_2$/Nb (x nm)/[Pt (0.9 nm)/Co (0.75 nm)]$_2$/Pt multilayers with different Nb thickness were deposited onto SiO$_2$/Si substrates using a DC magnetron sputtering system with a base pressure less than 1×10^{-7} Torr at room temperature. The Ar working pressure increased to 3 mT with a DC power of 20 W during the evaporation. An in-suit quartz crystal microbalance monitored the deposition rate. The temperature-dependent X-band (~9.3 GHz) FMR measurement was carried out via an electron paramagnetic resonance spectrometer (JES-FA200, JOEL) equipped with a variable temperature down to liquid helium temperature. The magnetic hysteresis loops were recorded for different temperatures by a superconducting quantum interference device (MPMS3, Quantum Design) in the DC scan mode.

III. RESULTS AND DISCUSSION

The Pt/(Co/Pt)$_2$/Nb/(Pt/Co)$_2$/Pt magnetic heterostructures with perpendicular magnetic anisotropy show an oscillating behavior between ferromagnetic and antiferromagnetic exchange coupling by controlling the thickness of the Nb interlayer. The film structure and the measurement geometry of FMR test are schematically depicted in Fig. 1(a). The FMR measurements are performed in an X-band (≈9.3 GHz) resonator cavity with the TE$_{011}$ mode. The external magnetic field is applied perpendicular to the film plane. The FMR spectra for different thicknesses of the Nb spacer layer are shown in Fig. 1(b). Strikingly, two resonance fields are observed in FMR spectra for all samples due to two different precession modes of magnetization vectors in the neighboring ferromagnetic layer. The in-phase precession and out-of-phase precession modes are the acoustic and optical spin-wave resonance modes, respectively. In the perpendicular magnetic anisotropy condition, the resonance field of the acoustic mode and optical mode along the easy axis can be expressed by the out-of-plane Kittle equation, including the effective

interlayer coupling field J_{eff} as follows:[25,26]

$$
\begin{aligned}
f_r &= \frac{\gamma}{2\pi}(H_{AM} + H_k - 4\pi M_{eff}), \\
f_r &= \frac{\gamma}{2\pi}(H_{OM} + J_{eff} + H_k - 4\pi M_{eff}),
\end{aligned}
\tag{1}
$$

where f_r is the resonance frequency and γ is the gyromagnetic ratio of 2.8 MHz/Oe. H_{AM} and H_{OM} represent the resonant field for acoustic mode and optical mode, respectively. J_{eff} is the distance between the resonance field of acoustic mode and optical mode called mode separation. J_{eff} is related to the exchange coupling energy J_{RKKY} as $J_{eff} = -2\frac{J_{RKKY}}{dM}$. Here, d is the thickness of a single ferromagnetic layer, and J_{RKKY} represents the RKKY coupling energy. Positive values of J_{RKKY} indicate ferromagnetic coupling, whereas negative values represent antiferromagnetic coupling.[27] The RKKY coupling energy oscillates and changes signs with the Nb spacer thickness at room temperature. The optical mode H_{OM} appears at a higher magnetic field than the acoustic mode H_{AM} in the ferromagnetic coupling condition (and vice versa). We distinguish the optical and acoustic modes by combining the FMR spectra and magnetic hysteresis loop results. Figure 1(c) shows the normalized magnetic hysteresis loops measured when the external magnetic field is perpendicular to the film. The hybridization between the 3d bands in the ferromagnetic layers and the conduction band in the spacer metal layer leads to an attenuated oscillatory of the exchange coupling with increasing spacer layer thickness.[28] The double S-shape hysteresis loop appears at Nb thickness varying from 1.7 to 2.0 nm, corresponding to the antiferromagnetic coupling behavior.[29] It is worth noticing that the sample inhomogeneity such as nanogranular magnets and domains may also cause the double S-shape hysteresis loop.[30,31] Conversely, a single-pattern hysteresis loop can be observed when the Nb layer thickness increases further over 2.1 nm, corresponding to the ferromagnetic coupling behavior. Figure 1(b) shows that the distance between the two kinds of resonance fields decreases first. It then increases with the increasing Nb thickness accompanied by the switching of ferromagnetic and antiferromagnetic exchange coupling. The spacer layer thickness-dependent J_{RKKY} is shown in Fig. 1(d). Based on the quantum interference model and RKKY model, the oscillating behavior of coupling energy J_{RKKY} can be expressed in a crude approximation below:[32,33]

$$
J_{RKKY} \propto \frac{1}{(2k_F t_s)^2} \sin(2k_F t_s),
\tag{2}
$$

where the t_s and k_F represent the thickness and Fermi wave vector of the spacer layer, respectively. As shown in Fig. 1(d), an oscillatory change of J_{RKKY} decaying with the spacer distance can be observed in the Pt/(Co/Pt)$_2$/Nb/(Pt/Co)$_2$/Pt multilayers. The black line symbolized the fitting results using Eq. (2) shows good consistency with the experiment results in two oscillation periods. The Fermi vector k_F of Nb derived from fitting the oscillatory behavior equals 2.93 ± 0.03 nm^{-1}, comparable to the previous reports.[33] The oscillatory exchange coupling as a function of Nb layer thickness shows a period of 5.5 Å in a reasonable value,[34] which again supports the existence of interlayer exchange coupling and the transition between
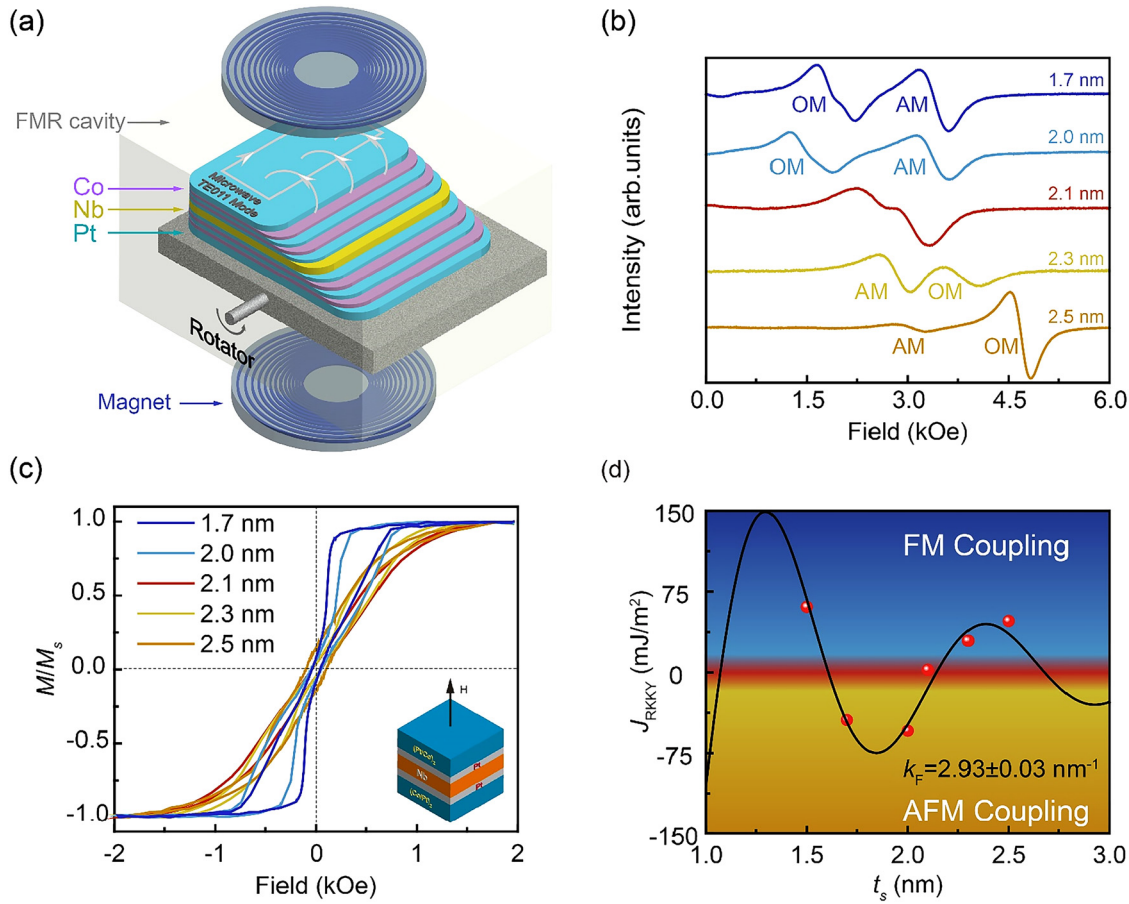
FIG. 1. Exchange coupling in Pt/(Co/Pt)$_2$/Nb/(Pt/Co)$_2$/Pt multilayers with different thicknesses of Nb. (a) Schematic of the FMR measurement geometry. (b) FMR absorption spectra of samples Pt/(Co/Pt)$_2$/Nb/(Pt/Co)$_2$/Pt with different Nb layer thicknesses. (c) Out-of-plane normalized magnetization loops of samples Pt/(Co/Pt)$_2$/Nb/(Pt/Co)$_2$/Pt with different Nb layer thicknesses. (d) Dependence of the RKKY coupling energy as a function of the Nb spacer layer thickness. The black line indicates the fitting result of oscillatory behavior.

antiferromagnetic and ferromagnetic ordering in Pt/(Co/Pt)$_2$/Nb/(Pt/Co)$_2$/Pt structures.

The temperature-dependent interlayer exchange coupling in the ferromagnetic coupling condition is determined using a 2.5 nm Nb spacer layer sample as shown in Fig. 2(a). The typical FMR spectra and the corresponding J_{RKKY} value vs different temperatures are demonstrated in Figs. 2(b) and 2(c), respectively. As expected for the theoretical analysis based on the pure temperature effect, the coupling increased with the temperature decreased, implying the enhanced exchange coupling at low temperature. Recall that in the free electron model for the energy dispersion, the intensity of RKKY interaction as a function of temperature can be expressed as

$$J_{RKKY} \propto - \left[\frac{\sin(2k_F t_s) - 2k_F t_s \cos(2k_F t_s)}{(k_F t_s)^4} - \frac{\pi^2}{3} \left(\frac{k_B T}{\varepsilon_F} \right)^2 \frac{\cos(2k_F t_s)}{k_F t_s} \right],$$

(3)

where ε_F is the Fermi energy and k_B represents the Boltzmann constant. Overall, we find that the theoretical fitting results shown in Fig. 2(c) are consistent with the experimental results, further demonstrating that the changing of coupling energy is due to the pure temperature effect. There are two prerequisites in investigating the interlayer exchange coupling mediated by the superconducting layer. On the one hand, a relatively thick Nb layer of about 20 nm is required at ultralow temperature to protect the superconducting state from the damage of inverse proximity effect.[35,36] On the other hand, the coupling strength of RKKY interaction decay inversely proportional to the square of distance. This property limits the thickness of the spacing layer in an ultrathin region, usually less than 5 nm. However, the superconducting transition of ultrathin Nb is easily suppressed by adjacent ferromagnetic layers via the inverse proximity effect. Such conflicting requirements make this problem more complicated.

Here in our works, the Nb layer is protected by the neighboring Pt layer without direct contact with the ferromagnetic Co layer.
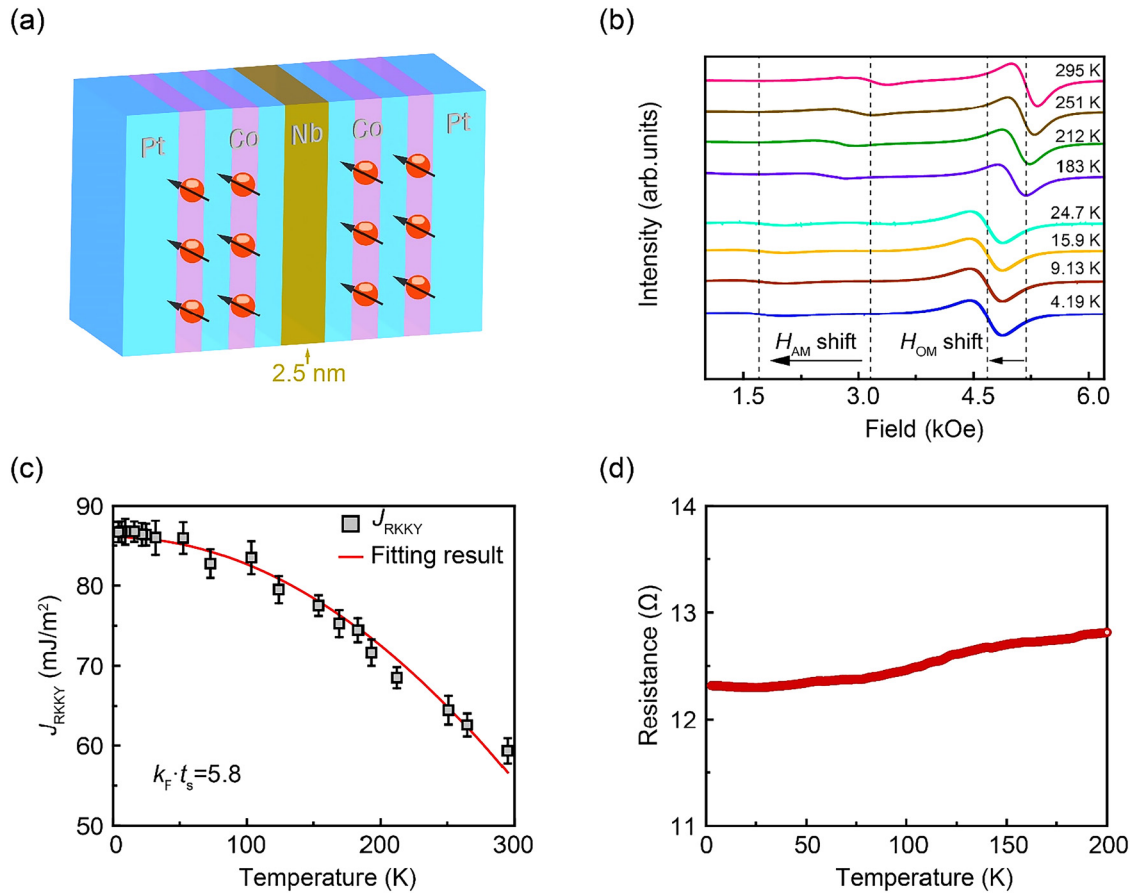
20 December 2024 07:55:19

FIG. 2. Temperature-dependent exchange coupling in the sample Pt/(Co/Pt)$_2$/Nb(2.5 nm)/(Pt/Co)$_2$/Pt with ferromagnetic coupling. (a) Schematic of the structure with ferromagnetic coupling. (b) Typical FMR spectra and (c) corresponding coupling strength J_{RKKY} as a function of temperature during the cooling process. The red line represents the fitting result using $(k_B T/\varepsilon_F)^2$ relationship. (d) The evolution of the temperature dependence of the sheet resistance.

So, the Co/Pt multilayers can suppress the inverse proximity effect and further reduce the inhibition of superconductivity order in the Nb layer to some extent. To directly characterize the superconducting properties of the spacer Nb layer, we have measured the temperature dependence of the sheet resistance, as shown in Fig. 2(d). The superconducting transition is not observed in the sample of Pt/(Co/Pt)$_2$/Nb (2.0 nm)/(Pt/Co)$_2$/Pt with ferromagnetic coupling states. The absence of superconducting transition here is probably due to the suppression from ferromagnetic coupling. The measured absence of superconducting transition is in apparent agreement with the results of temperature-dependent coupling energy, which further demonstrates the bare temperature effect in Pt/(Co/Pt)$_2$/Nb (2.5 nm)/(Pt/Co)$_2$/Pt.

However, a new spin-wave resonance mode emerges at an ultralow temperature around $k_B T < \Delta$[37] in the condition of a 2.0 nm Nb spacer layer with antiferromagnetic coupling as shown in Fig. 3(a). This phenomenon does not match the bare temperature effect, indicating the spin dynamic behavior is different from itinerant electrons mediated RKKY interaction. The typical FMR spectra

with different temperatures are illustrated in Fig. 3(b). The dynamic behavior in the temperature above 174 K exhibits a pure temperature effect. With the temperature decreasing from 300 to 174 K, the acoustic mode H_{AM} decreased around 150 Oe, while the optical mode H_{OM} remarkably decreased by about 470 Oe. Recall that the position of acoustic mode only depends on the intrinsic property of magnetic layer and is not affected by the interlayer exchange coupling. However, the position of optical mode is a complex condition affected by magnetic layer and coupling strength. Hence, those observations can be explained that H_k–$4\pi M_{eff}$ change relatively small than J_{eff} in decreasing temperature. The optical mode H_{OM} shows a dramatic shift owing to the temperature sensitivity of J_{eff}. The coupling energy J_{RKKY} as a function of temperature above 152 K is also in accord with the pure temperature effect, as shown in Fig. 3(d). Moreover, the fitting results of $k_F \cdot t_s$ value are determined to be 4.6. The ratio of $k_F \cdot t_s$ in ferromagnetic coupling states to antiferromagnetic coupling states is determined to be 1.26 and the ratio of Nb thickness is 1.25, which guarantees the self-consistent of the results. Figure 3(f)
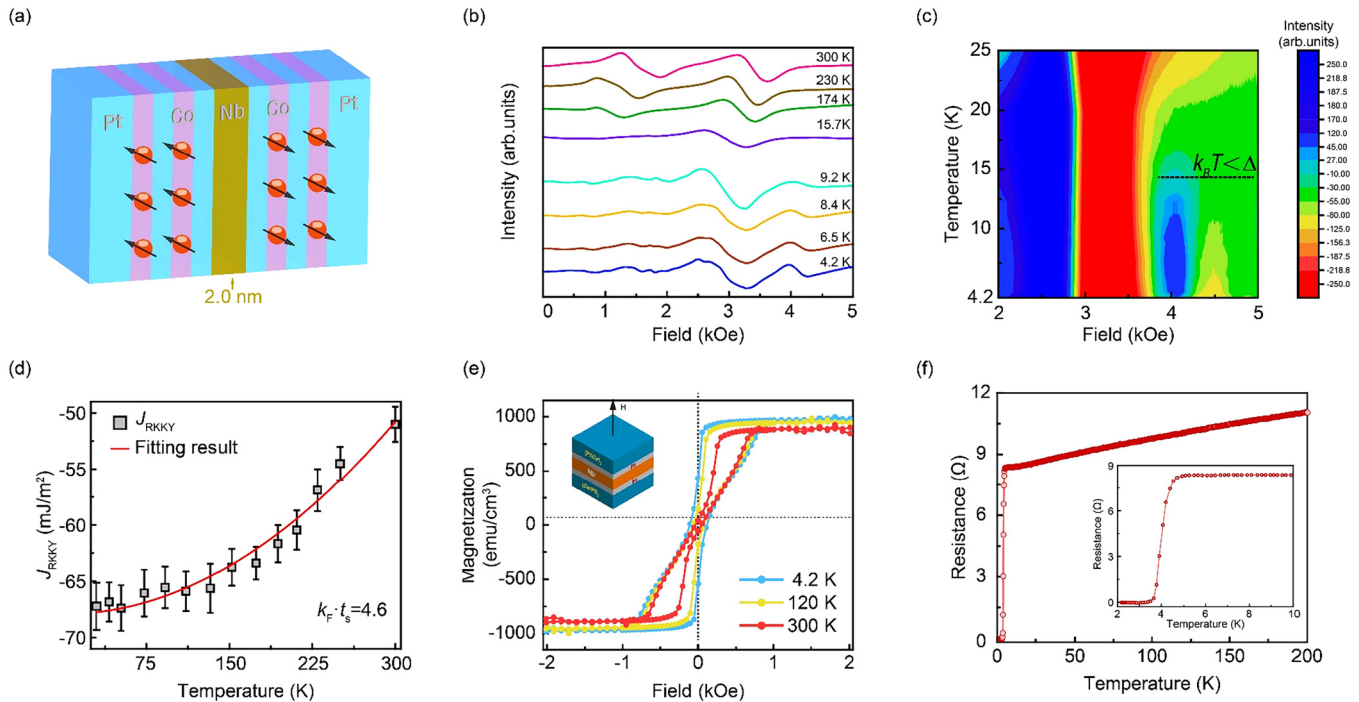
20 December 2024 07:55:19

FIG. 3. Temperature-dependent exchange coupling in the sample Pt/(Co/Pt)$_2$/Nb(2.0 nm)/(Pt/Co)$_2$/Pt with antiferromagnetic coupling. (a) Schematic of the structure with antiferromagnetic coupling. (b) Typical FMR spectra from room temperature to 4.2 K. (c) Detailed FMR phase diagram at ultralow temperature. The FMR intensity is plotted as a function of the external field and temperature scaled by the contour map. (d) The value of RKKY coupling energy as a function of temperature from room temperature to 150 K. The red line represents the fitting result using $(k_B T/\varepsilon_F)^2$ relationship. (e) Comparison of the out-of-plane magnetic hysteresis loops under 4.2, 120, and 300 K. (f) The sheet resistance as a function of temperature in the entire temperature range. The inset shows a detailed version in the region from 2 to 10 K.

demonstrates the temperature-dependent sheet resistance. Unlike the ferromagnetic coupling states, the antiparallel magnetization alignment in antiferromagnetic coupling states has little influence on the superconductive layer. Thus, the superconducting transition around 4 K can be observed.

In the ultralow temperature region, the acoustic mode remained almost unchanged over the temperature decreasing from 15.7 to 4.2 K due to the small temperature changes ΔT only around 10 K, as shown in the bottom part of Fig. 3(b). However, a new resonance field emerges around 4 kOe as the further temperature decreases around $k_B T < \Delta$. The FMR phase diagram in Fig. 3(c) provides a detailed overview, and a new resonance field emerged in the lower right corner. Combined with the optical mode resonance field around 1.2 kOe tends to vanish, a reversal of acoustic mode resonance field and optical mode resonance field is exhibited. Since the double S-shape hysteresis loop is retained, illustrated in Fig. 3(e), the overall coupling mode remains antiferromagnetic coupling unchanged. Here, the position of the new resonance field is different from the conventional antiferromagnetic coupling mode, implying the setup of an extra antiferromagnetic coupling channel.

In the superconductor/ferromagnet heterostructure, magnetic atoms are detrimental for Cooper pairs because they induce spin-polarized subgap states. The magnetism atoms locally or even completely break Cooper pairs and allow additional subgap bound states dubbed Yu–Shiba–Rusinov (YSR) bound states inside superconducting gaps. Apart from the conventional RKKY interaction, the YSR bound states of the two magnetic layers hybridize in a spin-dependent fashion, which results in a new coupling mechanism.[19,24] Unlike the RKKY, interaction induced by itinerant electrons can vary between ferromagnetic and antiferromagnetic coupling states. The YSR interaction only oscillates in the antiferromagnetic region to the physical limitations that the YSR contribution to the exchange only occurs for antialigned magnetization.

Figure 4(a) shows the schematic of the heterostructure and the overlap of the localized bound state, the so-called YSR interaction. The YSR interaction is expected to mediate strong exchange even dominated over conventional RKKY interaction when the distance t_s is smaller than the superconducting coherence length. To directly compare the spin dynamic behavior under RKKY and YSR interaction, we plot the FMR spectra under 300 and 4.2 K in Fig. 4(b). The sign of J_{eff} also depends on the phase difference $\Delta\varphi$ of the mediation particle described as follows:[38] $J_{eff} \propto J_{inter} \cos \Delta\varphi$. In the condition of antiferromagnetic coupling state, the phase difference of RKKY interaction mediated by itinerant electrons can be expressed as $\Delta\varphi_e = \pi$, while the phase difference of YSR interaction mediated by the Cooper pairs following $\Delta\varphi_{BCS} = 0$. This is probably the reason why the order of acoustic mode and optical mode reversed, as shown in Fig. 4(b). The YSR bound states that
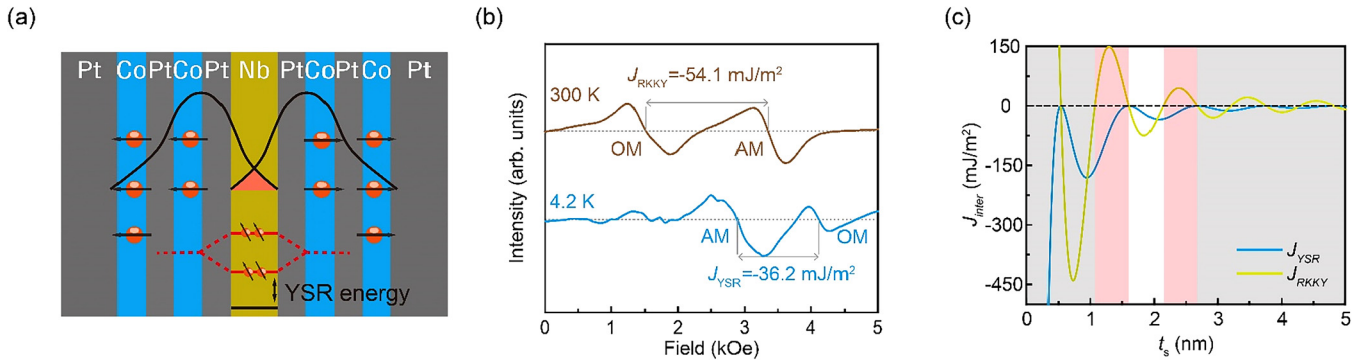
FIG. 4. YSR interaction in the structure of Pt/(Co/Pt)$_2$/Nb(2.0 nm)/(Pt/Co)$_2$/Pt at ultralow temperature. (a) Schematic of the antiferromagnetic interaction induced by the hybrid YSR states. (b) Comparison of FMR spectra of sample Pt/(Co/Pt)$_2$/Nb(2.0 nm)/(Pt/Co)$_2$/Pt under room temperature and 4.2 K with RKKY interaction and YSR-induced interaction, respectively. (c) Comparison of calculated coupling energy between RKKY interaction and YSR-induced interaction in Pt/(Co/Pt)$_2$/Nb/(Pt/Co)$_2$/Pt multilayers with different Nb spacing layer thicknesses.

contribute to the exchange energy can be expressed as[24]

$$J_{\text{YSR}} = -\Delta \frac{1}{1-\beta} \frac{\cos^2(k_F t_s)}{2(k_F t_s)^2} e^{-(2t_s/\xi)}, \quad (4)$$

where Δ represents the superconducting gap, ξ is the superconducting coherence length, and β is a value <1 related to the normal state DOS at the Fermi energy. The theoretical coupling energy of RKKY interaction and YSR interaction vs spacer layer thickness at $\beta = 0.997$ are presented in Fig. 4(c). The k_F parameter used in the calculation is 2.9 nm^{-1} derived from the fitting results in Fig. 1(c) to ensure comparability. For concreteness, the superconducting gap Δ is 1.2 meV, and ξ is 12 nm from the previous results. The theory of YSR interaction predicts that the coupling energy of the multilayer sample with 2 nm Nb spacing layer is around -32.6 mJ/m^2, which is comparable with the experiment result of about -36.2 mJ/m^2. Combining the behavior of FMR mode reversal and the quantitatively determined coupling energy, those features are distinctly different from the traditional RKKY interaction and are in good agreement with the prediction of YSR interaction.

IV. CONCLUSIONS

To conclude, an extra YSR interaction is observed in the Pt/(Co/Pt)$_2$/Nb/(Pt/Co)$_2$/Pt synthetic antiferromagnetic multilayers at ultralow temperature. Unlike conventional RKKY interaction, the YSR interaction results from the YSR bound states induced by the broken Cooper pairs. The observation of YSR interaction in synthetic antiferromagnetic multilayers promises opportunities for further discoveries in applying antiferromagnetic spintronic devices.

SUPPLEMENTARY MATERIAL

See the supplementary material for further angular dependent FMR measurements and mode separation of Pt/(Co/Pt)$_2$/Nb (2.0 nm)/(Pt/Co)$_2$/Pt multilayers.

AUTHOR DECLARATIONS

Conflict of Interest

The authors have no conflicts to disclose.

Author Contributions

Q.L. and Y.L. contributed equally to this work.

Qi Lu: Conceptualization (lead); Data curation (lead); Formal analysis (lead); Funding acquisition (equal); Resources (lead); Visualization (lead); Writing – original draft (lead). **Yaojin Li:** Methodology (lead); Resources (lead). **Tao Li:** Methodology (equal); Software (equal). **Tai Min:** Funding acquisition (equal); Resources (lead). **Zhuang-De Jiang:** Funding acquisition (lead); Investigation (lead). **Young Sun:** Methodology (lead); Resources (lead); Software (lead). **Ming Liu:** Conceptualization (lead); Funding acquisition (lead); Project administration (lead); Supervision (lead); Validation (lead); Writing – review & editing (lead).

DATA AVAILABILITY

The data that support the findings of this study are available from the corresponding author upon reasonable request.

20 December 2024 07:55:19

REFERENCES

[1]M. Kimata, H. Chen, K. Kondou, S. Sugimoto, P. K. Muduli, M. Ikhlas, Y. Omori, T. Tomita, A. H. MacDonald, S. Nakatsuji, and Y. Otani, "Magnetic and magnetic inverse spin Hall effects in a non-collinear antiferromagnet," Nature **565**, 627 (2019).

[2]A. Bose, N. J. Schreiber, R. Jain, D.-F. Shao, H. P. Nair, J. Sun, X. S. Zhang, D. A. Muller, E. Y. Tsymbal, D. G. Schlom, and D. C. Ralph, "Tilted spin current generated by the collinear antiferromagnet ruthenium dioxide," Nat. Electron. **5**, 267 (2022).

[3]W. Zhang, M. B. Jungfleisch, W. Jiang, J. E. Pearson, A. Hoffmann, F. Freimuth, and Y. Mokrousov, "Spin Hall effects in metallic antiferromagnets," Phys. Rev. Lett. **113**, 196602 (2014).

[4]X. Wu, H. Wang, H. Liu, Y. Wang, X. Chen, P. Chen, P. Li, X. Han, J. Miao, H. Yu, C. Wan, J. Zhao, and S. Chen, "Antiferromagnetic–ferromagnetic heterostructure-based field-free terahertz emitters," Adv. Mater. **34**, 2204373 (2022).

[5]X. Chen, S. Shi, G. Shi, X. Fan, C. Song, X. Zhou, H. Bai, L. Liao, Y. Zhou, H. Zhang, A. Li, Y. Chen, X. Han, S. Jiang, Z. Zhu, H. Wu, X. Wang, D. Xue, H. Yang, and F. Pan, "Observation of the antiferromagnetic spin Hall effect," Nat. Mater. **20**, 800 (2021).

[6]J. Dong, X. Li, G. Gurung, M. Zhu, P. Zhang, F. Zheng, E. Y. Tsymbal, and J. Zhang, "Tunneling magnetoresistance in noncollinear antiferromagnetic tunnel junctions," Phys. Rev. Lett. **128**, 197201 (2022).

[7]R. A. Duine, K. J. Lee, S. S. P. Parkin, and M. D. Stiles, "Synthetic antiferromagnetic spintronics," Nat. Phys. **14**, 217 (2018).

[8]S. S. P. Parkin, A. Mansour, and G. P. Felcher, "Antiferromagnetic interlayer exchange coupling in sputtered Fe/Cr multilayers: Dependence on number of Fe layers," Appl. Phys. Lett. **58**, 1473 (1991).

[9]P. A. Grünberg, "Nobel lecture: From spin waves to giant magnetoresistance and beyond," Rev. Mod. Phys. **80**, 1531 (2008).

[10]G. Zhang, T. Samuely, Z. Xu, J. K. Jochum, A. Volodin, S. Zhou, P. W. May, O. Onufriienko, J. Kačmarčík, J. A. Steele, J. Li, J. Vanacken, J. Vacik, P. Szabó, H. Yuan, M. B. J. Roeffaers, D. Cerbu, P. Samuely, J. Hofkens, and V. V. Moshchalkov, "Superconducting ferromagnetic nanodiamond," ACS Nano **11**, 5358 (2017).

[11]Y. Zhu, A. Pal, M. G. Blamire, and Z. H. Barber, "Superconducting exchange coupling between ferromagnets," Nat. Mater. **16**, 195 (2017).

[12]K. R. Jeon, C. Ciccarelli, A. J. Ferguson, H. Kurebayashi, L. F. Cohen, X. Montiel, M. Eschrig, J. W. A. Robinson, and M. G. Blamire, "Enhanced spin pumping into superconductors provides evidence for superconducting pure spin currents," Nat. Mater. **17**, 499 (2018).

[13]A. I. Buzdin, "Proximity effects in superconductor-ferromagnet heterostructures," Rev. Mod. Phys. **77**, 935 (2005).

[14]C. Bell, S. Milikisyants, M. Huber, and J. Aarts, "Spin dynamics in a superconductor-ferromagnet proximity system," Phys. Rev. Lett. **100**, 047002 (2008).

[15]L. Li, Y. Zhao, X. Zhang, and Y. Sun, "Possible evidence for spin-transfer torque induced by spin-triplet supercurrents," Chin. Phys. Lett. **35**, 077401 (2018).

[16]M. G. Flokstra, N. Satchell, J. Kim, G. Burnell, P. J. Curran, S. J. Bending, J. F. K. Cooper, C. J. Kinane, S. Langridge, A. Isidori, N. Pugach, M. Eschrig, H. Luetkens, A. Suter, T. Prokscha, and S. L. Lee, "Remotely induced magnetism in a normal metal using a superconducting spin-valve," Nat. Phys. **12**, 57 (2015).

[17]K. Ohnishi, S. Komori, G. Yang, K. R. Jeon, L. A. B. Olde Olthof, X. Montiel, M. G. Blamire, and J. W. A. Robinson, "Spin-transport in superconductors," Appl. Phys. Lett. **116**, 130501 (2020).

[18]M. Wachowiak, A. Marczyńska, H. Dawczak-Dębicki, M. Pugaczowa-Michalska, S. Pacanowski, Ł Majchrzycki, and L. Smardz, "Modification of exchange coupling in Fe/Nb/Fe/Pd layered structures using hydrogen," Acta Phys. Pol. **133**, 609 (2018).

[19]L. Yu, "Bound state in superconductors with paramagnetic impurities," Acta. Phys. Sin. **21**, 75 (1965).

[20]H. Shiba, "Classical spins in superconductors," Prog. Theor. Phys. **40**, 435 (1968).

[21]A. I. Rusinov, "On Theory of Gapless Superconductivity in Alloys Containing Paramagnetic Impurities," Sov. J. Exp. Theor. Phys. **29**, 1101 (1969).

[22]H. Müller, M. Eckstein, and S. Viola Kusminskiy, "Control of Yu-Shiba-Rusinov states through a Bosonic mode," Phys. Rev. Lett. **130**, 106905 (2023).

[23]G. Zhang, T. Samuely, N. Iwahara, J. Kačmarčík, C. Wang, P. W. May, J. K. Jochum, O. Onufriienko, P. Szabó, S. Zhou, P. Samuely, V. V. Moshchalkov, L. F. Chibotaru, and H. G. Rubahn, "Yu-Shiba-Rusinov bands in ferromagnetic superconducting diamond," Sci. Adv. **6**, eaaz2536 (2020).

[24]N. Y. Yao, L. I. Glazman, E. A. Demler, M. D. Lukin, and J. D. Sau, "Enhanced antiferromagnetic exchange between magnetic impurities in a superconducting host," Phys. Rev. Lett. **113**, 087202 (2014).

[25]S. Li, Q. Li, J. Xu, S. Yan, G.-X. Miao, S. Kang, Y. Dai, J. Jiao, and Y. Lü, "Tunable optical mode ferromagnetic resonance in FeCoB/Ru/FeCoB synthetic antiferromagnetic trilayers under uniaxial magnetic anisotropy," Adv. Funct. Mater. **26**, 3738 (2016).

[26]M. Liu, O. Obi, Z. H. Cai, J. Lou, G. M. Yang, K. S. Ziemer, and N. X. Sun, "Electrical tuning of magnetism in Fe_3O_4/PZN-PT multiferroic heterostructures derived by reactive magnetron sputtering," J. Appl. Phys. **107**, 073916 (2010).

[27]Y. Gong, Z. Cevher, M. Ebrahim, J. Lou, C. Pettiford, N. X. Sun, and Y. H. Ren, "Determination of magnetic anisotropies, interlayer coupling, and magnetization relaxation in FeCoB/Cr/FeCoB," J. Appl. Phys. **106**, 063916 (2009).

[28]P. Bruno and C. Chappert, "Oscillatory coupling between ferromagnetic layers separated by a nonmagnetic metal spacer," Phys. Rev. Lett. **67**, 1602 (1991).

[29]Q. Yang, L. Wang, Z. Zhou, L. Wang, Y. Zhang, S. Zhao, G. Dong, Y. Cheng, T. Min, Z. Hu, W. Chen, K. Xia, and M. Liu, "Ionic liquid gating control of RKKY interaction in FeCoB/Ru/FeCoB and $(Pt/Co)_2$/Ru/$(Co/Pt)_2$ multilayers," Nat. Commun. **9**, 991 (2018).

[30]F. Duc, J. Vanacken, G. Zhang, W. Decelle, J. E. Lorenzo, C. Detlefs, C. Strohm, T. Roth, R. Suryanarayanan, P. Frings, and G. L. J. A. Rikken, "Direct evidence of magnetostructural phase separation in the electron-doped manganite$Ca_{0.8}Sm_{0.16}Nd_{0.04}MnO_3$by means of high magnetic field studies," Phys. Rev. B **82**, 054105 (2010).

[31]G. Zhang, K. Potzger, S. Zhou, A. Mücklich, Y. Ma, and J. Fassbender, "Memory effect of magnetic nanoparticle systems originating from particle size distribution," Nucl. Instrum. Methods Phys. Res., Sec. B **267**, 1596 (2009).

[32]W. Baltensperger and J. S. Helman, "Ruderman–Kittel coupling between ferromagnets separated by a nonmagnetic layer," Appl. Phys. Lett. **57**, 2954 (1990).

[33]C. Rehm, F. Klose, D. Nagengast, H. Maletta, and A. Weidinger, "Magnetic coupling in Fe/Nb multilayers," Physica B **234**, 480 (1997).

[34]N. N. Shukla and R. Prasad, "Energy functional dependence of exchange coupling and magnetic properties of Fe/Nb multilayers," Phys. Rev. B **70**, 014420 (2004).

[35]J. Kim, Y.-J. Doh, K. Char, H. Doh, and H.-Y. Choi, "Proximity effect in Nb/Au/CoFe trilayers," Phys. Rev. B **71**, 214519 (2005).

[36]W. Han, S. Maekawa, and X. C. Xie, "Spin current as a probe of quantum materials," Nat. Mater. **19**, 139 (2019).

[37]D. Wang, J. Wiebe, R. Zhong, G. Gu, and R. Wiesendanger, "Spin-polarized Yu-Shiba-Rusinov states in an iron-based superconductor," Phys. Rev. Lett. **126**, 076802 (2021).

[38]J. Lindner and K. Baberschke, "Ferromagnetic resonance in coupled ultrathin films," J. Phys.: Condens. Matter **15**, S465 (2003).

20 December 2024 07:55:19